Virologica Sinica 38 (2023) 244–256

Contents lists available at ScienceDirect

Virologica Sinica

journal homepage: www.keaipublishing.com/en/journals/virologica-sinica
www.virosin.org

Research Article

An inactivated recombinant rabies virus chimerically expressed RBD induces humoral and cellular immunity against SARS-CoV-2 and RABV

Haili Zhang [a,1], Hongli Jin [a,c,1], Feihu Yan [b,1], Yumeng Song [a], Jiaxin Dai [a], Cuicui Jiao [a], Yujie Bai [a], Jingxuan Sun [a], Di Liu [c], Shen Wang [b], Mengyao Zhang [a], Jilong Lu [c], Jingbo Huang [a], Pei Huang [a], Yuanyuan Li [a], Xianzhu Xia [b], Hualei Wang [a,*]

[a] Key Laboratory of Zoonosis Research, Ministry of Education, College of Veterinary Medicine, Jilin University, Changchun, 130062, China
[b] Changchun Veterinary Research Institute, Chinese Academy of Agricultural Sciences, Changchun, 130122, China
[c] Changchun Sino Biotechnology Co., Ltd., Changchun, 130012, China

ARTICLE INFO

Keywords:
SARS-CoV-2
Vaccine
RBD
Chimeric expression
RABV

ABSTRACT

Many studies suggest that severe acute respiratory syndrome coronavirus 2 (SARS-CoV-2) can infect various animals and transmit among animals, and even to humans, posing a threat to humans and animals. There is an urgent need to develop inexpensive and efficient animal vaccines to prevent and control coronavirus disease 2019 (COVID-19) in animals. Rabies virus (RABV) is another important zoonotic pathogen that infects almost all warm-blooded animals and poses a great public health threat. The present study constructed two recombinant chimeric viruses expressing the S1 and RBD proteins of the SARS-CoV-2 Wuhan01 strain based on a reverse genetic system of the RABV SRV9 strain and evaluated their immunogenicity in mice, cats and dogs. The results showed that both inactivated recombinant viruses induced durable neutralizing antibodies against SARS-CoV-2 and RABV and a strong cellular immune response in mice. Notably, inactivated SRV-nCoV-RBD induced earlier antibody production than SRV-nCoV-S1, which was maintained at high levels for longer periods. Inactivated SRV-nCoV-RBD induced neutralizing antibodies against both SARS-CoV-2 and RABV in cats and dogs, with a relatively broad-spectrum cross-neutralization capability against the SARS-CoV-2 pseudoviruses including Alpha, Beta, Gamma, Delta, and Omicron, showing potential to be used as a safe bivalent vaccine candidate against COVID-19 and rabies in animals.

1. Introduction

Severe acute respiratory syndrome coronavirus 2 (SARS-CoV-2) is a β-coronavirus of *Coronaviridae* and the causative pathogen of coronavirus disease 2019 (COVID-19). SARS-CoV-2 is more contagious and harmful than other members of β-coronavirus, such as severe acute respiratory syndrome coronavirus (SARS-CoV) and Middle East respiratory syndrome (MERS-CoV). After the first case was reported in December 2019, the situation for COVID-19 has remained grim worldwide due to the continuous emergence of novel SARS-CoV-2 variants. In the absence of confirmed antiviral drugs for COVID-19, vaccines are undoubtedly the best means to form a herd immunity barrier to block virus transmission and reduce the mortality of patients. The COVID-19 vaccines were developed using different techniques (Maruggi et al., 2019; Gao et al., 2020; Lundstrom, 2020; Mulligan et al., 2020; van Doremalen et al., 2020; Wang et al., 2020; Yang et al., 2020; Zhu et al., 2020; Xia et al., 2021), and have played important roles in preventing the COVID-19 pandemic in humans.

After the emergence of SARS-CoV-2, some researchers speculated that the widespread of SARS-CoV-2 was achieved via intermediate mammalian hosts. Several studies have showed that SARS-CoV-2 infected a variety of animals in addition to humans, including common experimental animals such as ferrets, Syrian hamsters, crab-eating monkeys, and rhesus monkeys, and wild animals, such as minks, raccoon dogs, white-tailed deer, rabbits, Egyptian fruit bats, tigers, and lions (McAloose et al., 2020; Hoffmann et al., 2021). Even the most intimate human companion animals, such as pet dogs and cats, may be infected (Shi J. et al., 2020). Experimental studies showed that SARS-CoV-2 was transmissible between cats and minks via aerosols and contact (McAloose et al., 2020). Further studies showed that SARS-CoV-2 was transmissible across species

* Corresponding author.
E-mail address: wanghualei@jlu.edu.cn (H. Wang).
[1] Haili Zhang, Hongli Jin and Feihu Yan contributed equally to this work.

https://doi.org/10.1016/j.virs.2022.12.006
Received 12 September 2022; Accepted 26 December 2022
Available online 29 December 2022

in some animals. For example, minks transmitted the virus to farm cats and dogs through contact (Kim et al., 2020) and to humans to cause human-to-human transmission after mutation (Munnink et al., 2021).

Recent studies showed that SARS-CoV-2 variants could be transmitted back to humans from pet hamsters with subsequent community transmission events (Chan et al., 2022; Yen et al., 2022) and from pet cats to veterinary workers with morbidity (Sila et al., 2022). All of these studies indicate that with the continuous emergence of novel SARS-CoV-2 variants, animals infected with the variants may transmit the virus back to humans and pose a certain threat to humans and animals. Based on the concept of "One Health" for the correlation among human, animal and environmental health, we should attach importance to animals for their roles in SARS-CoV-2 transmission and the global pandemic, and develop efficient and inexpensive animal vaccines to prevent the outbreak of COVID-19 in animals.

Rabies virus (RABV) SRV9 strain was purified from the SAD strains and has been used as a vector to develop many kinds of animal vaccines (Zhang et al., 2019; Li et al., 2020; Jin et al., 2021; Chi et al., 2022). In this study, we employed the reverse genetic system of RABV SRV9 strain to construct recombinant RABVs chimeric expressing S1 protein and RBD protein of SARS-CoV-2, respectively, and evaluated their immunogenicity in mice, dogs and cats. The results showed that the inactivated recombinant viruses could effectively induce the body to produce efficient and durable neutralizing antibodies against both SARS-CoV-2 and RABV, which has the potential to be used as the effective vaccine in animals.

2. Materials and methods

2.1. Virus, cells and plasmids

The SARS-CoV-2 Wuhan01 strain was originally isolated from a COVID-19 patient in Wuhan (BetaCov/Wuhan/AMMS01/2020). Vesicular stomatitis virus (VSV)-vectored pseudoviruses expressing the intact S protein of SARS-CoV-2 Wuhan01 and variants of concern (VOCs), including Alpha, Beta, Gamma, Delta, and Omicron, were generated and stored in a Biosafety Level 3 (BSL-3) Laboratory (Wang et al., 2022; Yan et al., 2022). BSR cells, mouse neuroblastoma N2a cells (NA) and Vero E6 cells were cultured in Dulbecco's modified Eagle's medium (DMEM, Gibco, USA) with 10% fetal bovine serum (FBS, Gibco, USA) and 1% penicillin and streptomycin (P/S, Gibco, USA) at 37 °C in 5% CO_2. Suspended hamster kidney cells (BHK-21) were cultured in CD BHK-21 Production Medium (Thermo Fisher Scientific, USA) with 1% FBS and 0.5% penicillin/streptomycin at 37 °C under rotation at 120 rpm (Jin et al., 2021). The plasmid pD-SRV9-PM-TMCD containing the full-length cDNA of SRV9 and the helper plasmids (pD-N, pD-P, pD-M, and pD-G) required for the rescue of recombinant viruses were stored in our laboratory (Wang et al., 2015). The plasmid containing the *S* gene of SARS-CoV-2 was generated by gene synthesis (Sangon Biotech, China) according to the sequence of SARS-CoV-2 Wuhan01 strain (NC_045512.2) retrieved from GenBank.

2.2. Construction and rescue of the recombinant viruses

The primers for *S1* and the *receptor-binding domain (RBD)* were designed using Primer Premier software according to a construction strategy described previously (Jin et al., 2021). All of the primer details were provided in Supplemental Table S1. The *S1* gene was amplified from S-containing plasmids and inserted into the pD-SRV9-PM-TMCD plasmid via restriction sites *Bsi*WI and *Pac*I to construct the recombinant plasmid pD-SRV9-PM-S1-TMCD. For the *RBD* gene, two rounds of PCR amplification were used to introduce the signal peptide of the *S1* gene into its 5′ end to assist expression of the RBD protein on the surface of recombinant virus particles. The amplified products of the *RBD* gene were cloned into pD-SRV9-PM-TMCD by the same manner as *S1* to construct the recombinant plasmid pD-SRV9-PM-RBD-TMCD. The recombinant plasmids were identified by sequencing. The recombinant viruses SRV-nCoV-S1 and SRV-nCoV-RBD were rescued as described previously (Wang et al., 2015; Jin et al., 2021). Briefly, the recombinant plasmids pD-SRV9-S1-TMCD and pD-SRV9-RBD-TMCD were co-transfected with helper plasmids into BSR cells. Then the cell supernatants were harvested and passaged on NA cells. The recombinant viruses were subsequently identified by RT-PCR and sequencing.

2.3. Immunofluorescence analysis

NA cells were infected with the recombinant viruses at a multiplicity of infection (MOI) of 0.3, fixed with 4% paraformaldehyde (PFA) at 48 h post-infection, and permeabilized with or without 0.2% Triton X-100. The cells were blocked with 1% BSA for 30 min at 20–25 °C and incubated with a rabbit anti-SARS-CoV-2 RBD polyclonal antibody (PAb) (40592-T62, Sino Biological, 1:200) and mouse anti-RABV-G monoclonal antibody (mAb) (MAB8727, Abcam, 1:200) at 37 °C for 1 h. An FITC-conjugated anti-rabbit antibody (ab6717, Abcam, 1:300) and TRITC-conjugated anti-mouse antibody (T5393, Sigma, 1:500) were added and then incubated at 37 °C for 1 h. After staining with 4,6-diamidino-2-phenylindole (DAPI), the fluorescence was observed by confocal laser microscopy.

2.4. Electron microscopy analysis

The recombinant viruses were inactivated by treatment with ultraviolet (UV) light for 30 min. The samples were prepared as described previously (Jin et al., 2021) and observed by electron microscopy. To confirm the presence of the target proteins on viral particles, the samples were incubated with a mouse anti-RABV G mAb (1:50) and a rabbit anti-SARS-CoV-2 RBD PAb (1:50) for 1 h at 20–25 °C. Then the samples were stained with donkey anti-mouse IgG (ab39593, 10 nm gold, 1:20) and donkey anti-rabbit IgG (ab105296, 18 nm gold, 1:20) and observed by electron microscopy.

2.5. Growth kinetics and genetic stability of the recombinant viruses

BHK-21 suspension cells were infected with the recombinant viruses at different MOIs of 0.1, 0.5 and 1, and suspended at 37 °C in 5% CO_2 at 120 rpm for 96 h. The cell cultures were harvested every 24 h post-infection. The virus titers were determined in NA cells as described previously (Jin et al., 2021). The recombinant viruses were continuously passaged in suspended BHK-21 cells, and the supernatants and cells were collected every five passages for subsequent virus titration and genetic stability detection. The viral titers of recombinant viruses were detected by a previously described method (Jin et al., 2021) and calculated according to the Reed-Muench method (Muench and Reed, 1938; Ahmad et al., 2017; Lourenc Correia Moreira et al., 2019; Liu et al., 2020). The identified recombinant viruses were purified by a previously described method (Jin et al., 2021).

2.6. SDS-PAGE and Western blot analysis

The purified viruses were denatured and analyzed by sodium dodecyl sulfate (SDS)-polyacrylamide gel electrophoresis (PAGE). The gels were stained with Coomassie brilliant blue for total protein analysis. For Western blot (WB) analysis, the separated proteins were transferred onto nitrocellulose (NC) membranes and incubated with a rabbit anti-SARS-CoV-2 RBD protein PAb (1:2000) or rabbit anti-SARS-CoV-2 S1 protein PAb (40150-T62-COV2, Sino Biological, 1:2000). The membranes were incubated with a horseradish peroxidase (HRP)-conjugated goat anti-rabbit IgG antibody (ab6721, Abcam, 1:5000) for 1 h at 20–25 °C. Electrochemiluminescence (ECL) Western blotting Substrate (Pierce, USA) was added, and the bands were captured by a Tanon-5200 Chemiluminescent Imaging System (Tanon, China).

2.7. Immunizations in mice

The recombinant viruses were inactivated by treatment with β-propiolactone at a ratio of 1:3000. The inactivated recombinant viruses ($10^{9.05}$ $TCID_{50}$/mL) were mixed with poly(I:C) (Sigma, USA) at a final concentration of 0.2 mg/mL then mixed with ISA 201VG adjuvant (Seppic, France) in a volume ratio of 45:55. The mixture was emulsified and used for animal immunization experiments. The 6- to 8-week-old BALB/c mice were randomly divided into three groups with 17 mice in each group. The mice were immunized intramuscularly with 100 μL of vaccines as described above, or 100 μL of PBS mixed with ISA 201VG adjuvant and poly (I:C). The mice received three immunizations in total, separated by 2-week intervals. The sera were collected at 0, 2, 4, 6, 8, 12, 16 weeks post first immunization.

2.8. Anti-SARS-CoV-2 IgG detection and antibody isotype assay

A 96-well microtiter plate (Costar, USA) was coated with 0.5 μg per well of the recombinant SARS-CoV-2 RBD protein (Gene Universal, USA) in coating buffer (50 mmol/L Na_2CO_3, pH 9.6) and incubated overnight at 4 °C. Serum was diluted 200-fold with blocking buffer, added and processed as described previously (Jin et al., 2022). The results are reported as the positive index (ratio of sample OD_{450} to control OD_{450}) (Andrianaivoarimanana et al., 2012; Phillips et al., 2018; Jin et al., 2022).

2.9. Neutralization assay

Neutralizing titers of mouse sera were determined using the authentic SARS-CoV-2 Wuhan01 strain. Briefly, mouse sera were serially diluted in DMEM and incubated with an equal volume of SARS-CoV-2 containing 100 tissue culture-infecting dose 50 ($TCID_{50}$). After incubation at 37 °C for 1 h, aliquots were added to 50 μL of 1×10^4 Vero E6 cells in 96-well plates. The cells were observed daily for the presence or absence of virus-caused cytopathic effect (CPE) and recorded at 3 days post-infection (dpi) under a microscope. The serum neutralizing antibody titer was defined as the reciprocal of the highest dilution showing a 100% CPE reduction compared to the virus control. Virus-only controls and cell-only controls were included in each plate.

The cross-neutralizing titers of mouse, cat, and dog sera against SARS-CoV-2 VOCs (Alpha, Beta, Gamma, Delta and Omicron) were measured using a pseudovirus-based neutralizing assay. Briefly, serum samples were diluted from 1:10 with a serial twofold dilution in 96-well plates. VSV vectored pseudoviruses (50 μL, 100 $TCID_{50}$) were added to each serum dilution in duplicate. After 1 h of incubation at 37 °C and 5% CO_2, 50 μL of 1×10^4 Vero E6 cells was added to each well of the virus-serum mixture. The mixture was incubated for 48 h, and the CPE was read by fluorescent development detection under a fluorescence microscope. The serum neutralizing antibody titer was defined as the reciprocal of the highest dilution showing a 100% CPE reduction compared to the virus control.

For the detection of RABV-neutralizing antibodies, a fluorescent antibody virus neutralization (FAVN) test (Cliquet et al., 1998), which is a gold standards recommended by the World Organization for Animal Health (WOAH), was performed as previously described (Jin et al., 2021).

2.10. Flow cytometry

For dendritic cell (DC) and B-cell detection, the inguinal lymph nodes (LNs) were collected at 3, 6, and 9 days after the first immunization. A single-cell suspension was prepared in FACS buffer (PBS with 2% FBS) and seeded in a 96-well U-bottom plate at 5×10^5 cells/well. The cells were stained with antibodies against CD11c (PE-Cy7), CD80 (APC), MHC II (PerCP-CY5.5), CD19 (PerCP-Cy5.5), and CD69 (PE-Cy7) at 4 °C for 30 min. The cells were washed twice and examined by a FACSCalibur flow cytometer (BD Biosciences, USA).

For the detection of central memory T (TCM) cells, the spleens were collected at one week after the third immunization. Splenocytes were prepared as previously described (Jin et al., 2021) and suspended in RPMI 1640. A total of 2.5×10^5 splenocytes were seeded in 96-well U-bottom plates and stimulated with the purified SARS-CoV-2 RBD protein (10 μg/well). After co-culture for 48 h, the cells were stained with antibodies against CD4 (FITC), CD8 (PE), CD62L (Percy-cy5.5), and CD44 (APC) at 4 °C for 30 min and examined by a FACSCalibur flow cytometer.

2.11. ELISpot assay

A total of 5×10^5 splenocytes prepared above were seeded into ELISpot plates (Mabtech, Sweden) and stimulated with the purified SARS-CoV-2 RBD protein (10 μg/well). After incubation at 37 °C for 24 h, the plates were washed 5 times with PBST and incubated with biotin-labelled anti-interferon (IFN)-γ and anti-interleukin (IL)-4 antibodies (1:1000) (provided by the ELISpot kits) for 2 h at RT. The plates were washed and incubated with streptavidin-conjugated HRP (1:1000) for 1 h at RT. After the TMB substrate was added, the spot-forming cells (SFCs) in the plates were counted by an ELISpot reader (Multispotreader Spectrum, Germany).

2.12. ELISA-based measurement of cytokines

A total of 5×10^5 splenocytes were cultured in 96-well plates and stimulated with purified SARS-CoV-2 RBD protein (10 μg/well). After incubation for 72 h, the supernatants were harvested and centrifuged to remove cell fragments. The levels of cytokines including IL-2, tumor necrosis factor alpha (TNF-α), IFN-γ, IL-4, IL-5, IL-6, and IL-10, were detected by a Meso Scale Discovery (MSD) kit.

2.13. Immunizations in cats and dogs

The inactivated recombinant virus SRV-nCoV-RBD ($10^{9.05}$ $TCID_{50}$/mL) was mixed with Gel 02 adjuvant (SEPPIC, Paris, France) at a ratio of 7:1 to prepare the vaccine. Healthy adult cats were randomly assigned to two groups (n = 3/group). The cats were immunized subcutaneously with 1 mL of vaccine or PBS with Gel 02 adjuvant. Booster immunization was performed by subcutaneously administration of the same dose of vaccine or adjuvant 3 weeks after the first immunization. Serum samples were collected at 0, 3, 6, 8, and 13 weeks. Healthy adult dogs were randomly assigned to two groups (n = 5/group) and immunized subcutaneously with 1 mL of vaccine or PBS with Gel 02 adjuvant. Booster immunization was performed 3 weeks later. The sera were collected from the dogs at 0, 3, 5, 7, 9 and 11 weeks. The fecal production, behavior, and food and water consumption of cats and dogs were observed continuously throughout the experiments. The levels of IgG antibody against the SARS-CoV-2 RBD, and neutralizing antibodies against SARS-CoV-2 and RABV in serum were measured.

2.14. Statistical analysis

Statistical analyses were performed in GraphPad Prism (v9; GraphPad Software). Statistical differences between groups were assessed by one-way analysis of variance (ANOVA), followed by Dunnett's posttest. All experiments were performed independently with three biological replicates. Error bars represent standard deviations (SD) in each group (*, $P < 0.05$; **, $P < 0.01$; ***, $P < 0.001$; ****, $P < 0.0001$).

3. Results

3.1. Construction and identification of the recombinant viruses

The recombinant plasmids pD-SRV9-S1-TMCD and pD-SRV9-RBD-TMCD were constructed (Fig. 1A). The recombinant viruses SRV-nCoV-S1 and SRV-nCoV-RBD were rescued, and the expression of target

proteins was detected by a confocal microscopy assay. The results showed that when the cell membrane was permeabilized, RABV G and foreign proteins were detected in the cells infected with the recombinant viruses SRV-nCoV-S1 and SRV-nCoV-RBD, and RABV G was detected in cells infected with wild-type RABV (wt-RABV) (Fig. 1B). RABV G and the foreign protein of SARS-CoV-2 colocalized on the cell membrane when the infected cells were not permeabilized (Fig. 1B), which indicated that SARS-CoV-2 S1 and RBD proteins were expressed well and secreted to the cell membrane by the recombinant viruses.

The viruses were purified and analyzed by SDS-PAGE and WB to verify the chimeric expression of the foreign proteins in recombinant viruses. The SDS-PAGE results showed that the expected protein bands (approximately 120 kDa for the S1 protein and approximately 50 kDa for RBD protein) were found in recombinant viruses, with five structural proteins [nucleoprotein (N), phosphoprotein (P), matrix protein (M), glycoprotein (G), and RNA-dependent RNA polymerase (L), as indicated in the figure] of RABV found in all groups (Fig. 1C). The specific bands of the S1 protein and RBD protein were detected in the recombinant viruses

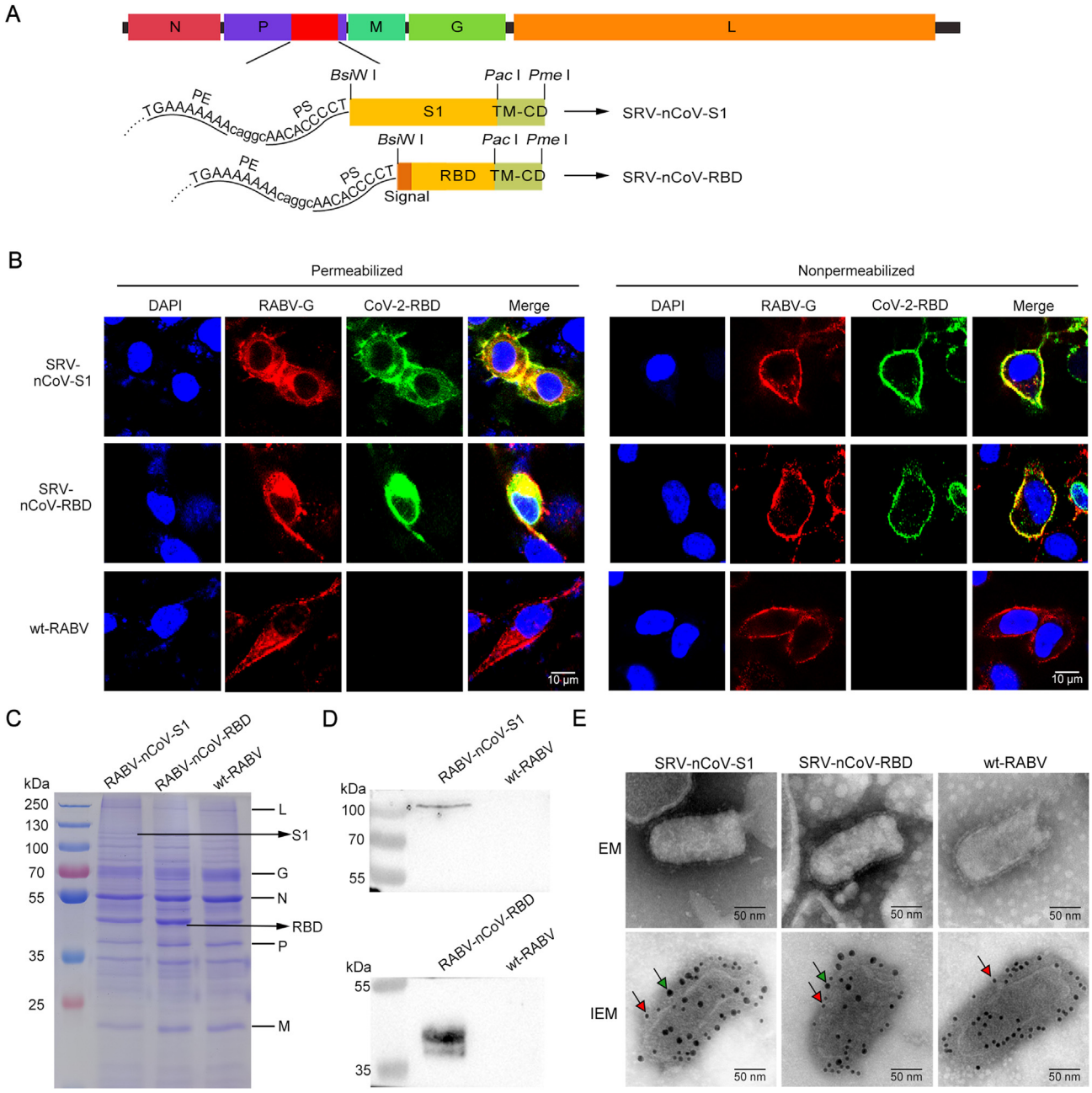

Fig. 1. Construction and identification of the recombinant viruses. **A** The construction scheme of the recombinant viruses SRV-nCoV-S1 and SRV-nCoV-RBD based on the reverse genetic operating system of RABV SRV9. **B** NA cells were infected with SRV-nCoV-S1, SRV-nCoV-RBD or wt-RABV SRV9. The cells were permeabilized or not at 48 h post-infection and then immunostained with antibodies against RABV G protein (red fluorescence) and SARS-CoV-2 RBD protein (green fluorescence). The nuclei were stained with DAPI (blue fluorescence). Scale bar: 10 μm. **C** The sucrose density gradient centrifugation-purified virions of recombinant viruses and wt-RABV SRV9 were analyzed by SDS-PAGE. The RABV proteins (RNA-dependent RNA polymerase (L), glycoprotein (G), nucleoprotein (N), phosphoprotein (P), and matrix protein (M)) and the S1 and RBD protein of SARS-CoV-2 were indicated on the corresponding bands. **D** Sucrose-purified virions were used to detect the expression of the exogenous proteins SARS-CoV-2 S1 and RBD. **E** Electron microscopy (EM) and dual-label immunogold EM detection of recombinant viruses. Gold particles (10 nm, red arrow) were used to label RABV G, and gold particles (18 nm, green arrow) were used to label the SARS-CoV-2 RBD protein. Scale bars represent 50 nm.

by WB analysis (Fig. 1D). These results suggested that the recombinant viruses SRV-nCoV-S1 and SRV-nCoV-RBD successfully chimerically expressed the S1 protein and RBD protein of SARS-CoV-2, respectively. To further detect whether the expression of exogenous protein affected the spatial structure of the recombinant RABVs, the recombinant viruses were negatively stained and observed by electron microscopy. As shown in Fig. 1E, the typical bullet shape of viral particles was observed in both recombinant viruses and wt-RABV, indicating that the expression of the exogenous proteins did not affect the assembly of RABV (Fig. 1E). Dual-labelling immunogold electron microscopy was used to detect the foreign proteins expressed on the surface of the viruses. The results showed that the recombinant viruses were labelled by both 10-nm gold particles (anti-RABV G) and 18-nm gold particles (anti-SARS-CoV-2 RBD), and the wt-RABV was only labelled by the 10-nm gold particles (Fig. 1E), which is consistent with the confocal and WB results. These results indicated that the S1 and RBD of SARS-CoV-2 proteins were successfully expressed on the viral particle surface by the recombinant viruses constructed in this study.

3.2. Growth characteristics of the recombinant viruses

Suspended BHK-21 cells were infected with the recombinant viruses at various MOIs to measure the viral growth kinetics. The titers of recombinant viruses were initially proportional to the MOI, i.e., the viral titers were increased with the increasing MOIs of the infected cells. The viral titers peaked on the 3rd day post-infection (up to $10^{8.97}$ $TCID_{50}$/mL for SRV-nCoV-S1 and SRV-nCoV-RBD) (Fig. 2A and B). Comparison of the growth kinetics of the recombinant viruses and wt-RABV added at an MOI of 0.5 showed that the recombinant viruses SRV-nCoV-S1 and SRV-nCoV-RBD had growth kinetics similar to wt-RABV (Fig. 2C), indicating that the chimeric expression of foreign proteins did not affect the growth kinetics of the recombinant viruses.

To confirm the genetic stability of the foreign genes inserted into the genome of RABV, the recombinant viruses were passaged continuously, the viral titers of the P5/P10/P15 viruses were determined and the target genes were amplified by RT-PCR. The results showed that the recombinant viruses could be passaged stably with the foreign genes and at high titers (Fig. 2D).

3.3. Inactivated recombinant viruses induced humoral immunity to RABV and SARS-CoV-2 in mice

To determine the immunogenicity of the recombinant viruses in mice, BALB/c mice were immunized intramuscularly with the inactivated recombinant viruses SRV-nCoV-S1 and SRV-nCoV-RBD, or PBS mixed with adjuvant and poly(I:C) at the indicated time points. The samples from mice, including sera, lymph nodes, and spleens, were collected at the indicated time points post-immunization for further analysis (Fig. 3A). Indirect ELISA was used to detect the level of antibodies in mouse sera, and the results showed that IgG antibodies against SARS-CoV-2 RBD protein were induced in the groups immunized with the inactivated SRV-nCoV-S1 and SRV-nCoV-RBD viruses. The level of IgG antibodies against SARS-CoV-2 RBD protein in mouse sera was increased after booster immunization, and the antibodies lasted at least 16 weeks after the first immunization (Fig. 3B). The IgG antibodies against the RBD protein induced by the inactivated SRV-nCoV-RBD appeared earlier and lasted longer than that of SRV-nCoV-S1, and the antibody titers of the SRV-nCoV-RBD group were significantly higher than those of SRV-nCoV-S1 group at the late stage after immunization (8-, 12-, and 16-week after the first immunization). The ratio of IgG2a (Th1-associated) to IgG1 (Th2-associated) in mouse sera was further analyzed to evaluate the type of immune response induced by the different viruses. The results showed that inactivated SRV-nCoV-RBD elicited a Th1/Th2-balanced immune response, and inactivated

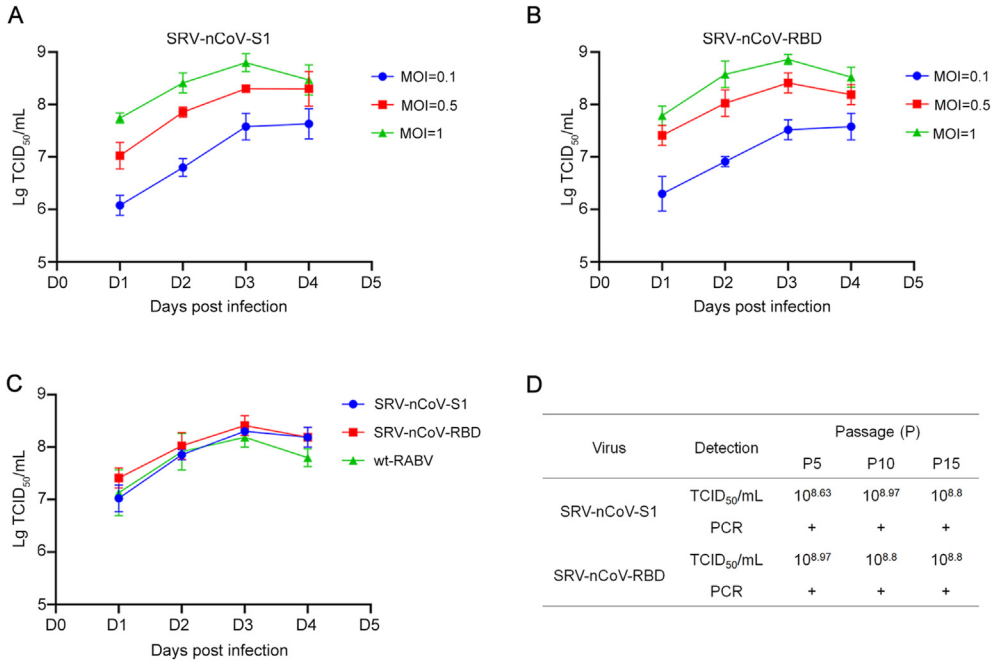

D

Virus	Detection	Passage (P)		
		P5	P10	P15
SRV-nCoV-S1	$TCID_{50}$/mL	$10^{8.63}$	$10^{8.97}$	$10^{8.8}$
	PCR	+	+	+
SRV-nCoV-RBD	$TCID_{50}$/mL	$10^{8.97}$	$10^{8.8}$	$10^{8.8}$
	PCR	+	+	+

Fig. 2. Growth kinetics and genetic characterization of the recombinant viruses SRV-nCoV-S1 and SRV-nCoV-RBD. **A**–**B** Suspended BHK21 cells were infected with SRV-nCoV-S1 or SRV-nCoV-RBD at an MOI of 0.1, 0.5 or 1. The samples were collected at days 1, 2, 3 and 4 post-infection, and the RABV titers were determined in NA cells. **C** The growth kinetics of the recombinant viruses were compared with RABV SRV9 at an MOI of 0.5. **D** The titers of recombinant viruses of different passages were determined, and the *S1* and *RBD* genes in recombinant viruses were identified by PCR and sequencing. All of these experiments were repeated 3 times independently.

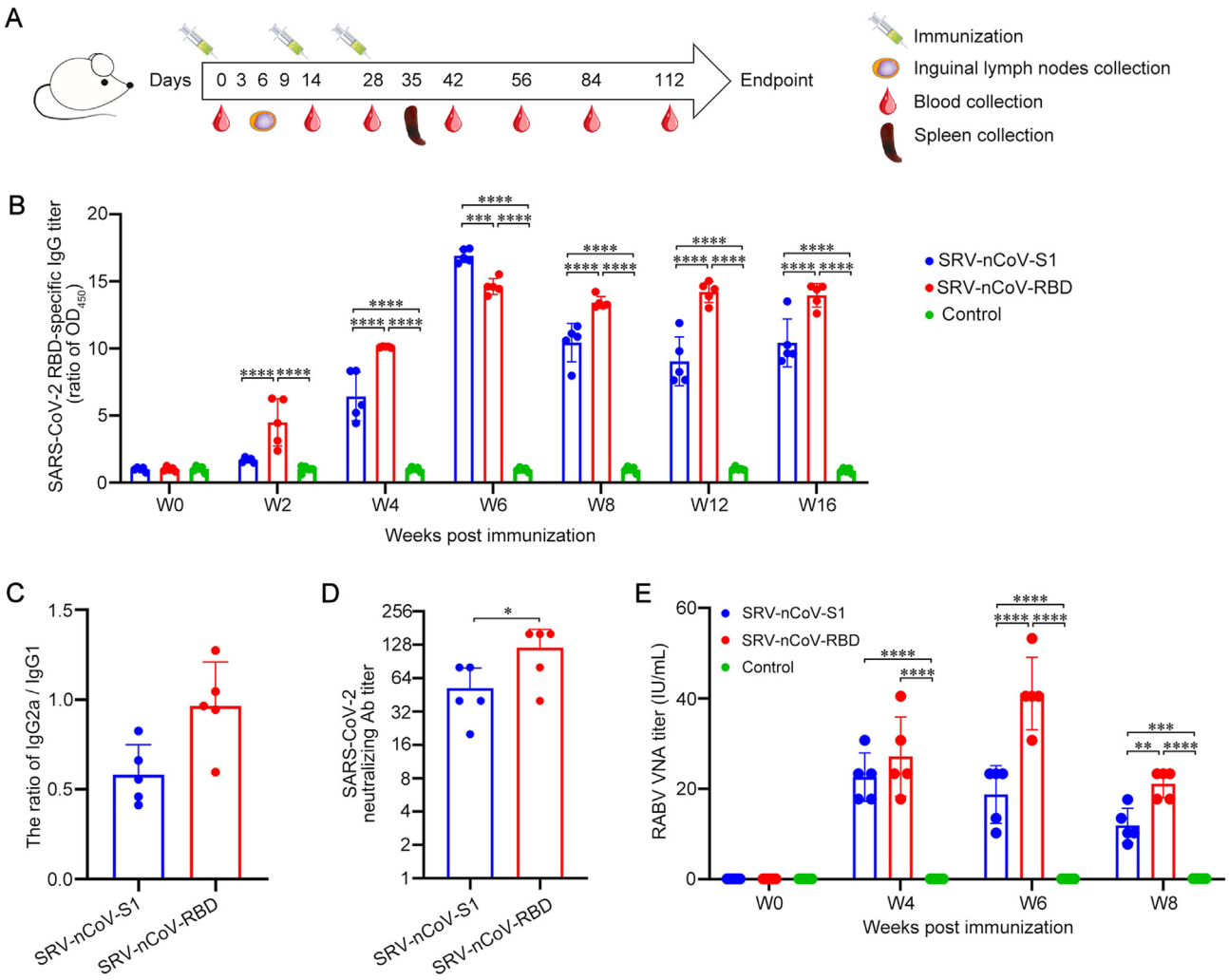

Fig. 3. Inactivated recombinant viruses induced humoral immunity to RABV and SARS-CoV-2 in mice. **A** Schematic of the immunization strategy in mice. The 6- to 8-week-old BALB/c mice (n = 17/group) were immunized intramuscularly with three doses of inactivated SRV-nCoV-S1 (20 μg), SRV-nCoV-RBD (20 μg), or PBS combined with an adjuvant complex of ISA 201 VG and poly(I:C) at 2-week intervals. Blood samples (n = 5/group) were collected on days 0, 14, 28, 56, 84 and 112. The inguinal lymph nodes (n = 3/group/day) were collected on days 3, 6, and 9. The spleens (n = 3/group) were collected on day 35. **B** SARS-CoV-2 RBD-specific IgG titers of mouse sera (n = 5/group) were detected by indirect ELISA with the purified RBD protein and were displayed as the ratio of sample/control OD_{450}. **C** IgG2a/IgG1 ratios of SARS-CoV-2 RBD-specific antibodies at week 6 post-immunization were assessed by indirect ELISA with the purified RBD protein. **D** The neutralizing antibody titers against the authentic SARS-CoV-2 Wuhan01 strain in mouse sera from different immunization groups (n = 5/group) at week 6 post-immunization were determined by a standard method. **E** RABV-neutralizing antibody titers of mouse sera at weeks 0, 4, 6, and 8 post-immunization were determined by the FAVN test. Data are presented as the means ± SD for each group. $^{*}P < 0.05$; $^{**}P < 0.01$; $^{***}P < 0.001$; $^{****}P < 0.0001$.

SRV-nCoV-S1 induced a Th2-biased immune response (Fig. 3C). To further evaluate the neutralization titers of antibodies induced by different recombinant viruses, we collected mouse sera at 6 weeks after immunization and tested their neutralization efficiency against the authentic SARS-CoV-2 Wuhan01 strain. Sera from the immunization groups showed neutralization of the Wuhan01 strain at titers greater than 1:80. The inactivated SRV-nCoV-RBD induced higher neutralization antibody titers than SRV-nCoV-S1 group (Fig. 3D).

Virus-neutralizing antibodies (VNAs) against RABV in mouse sera were detected by the FAVN method. The results suggested that the titers of VNAs induced by inactivated SRV-nCoV-S1 and SRV-nCoV-RBD were much higher than the standard 0.5 international unit (IU)/mL level considered protective (Shiota et al., 2009), indicating that SRV-nCoV-S1 and SRV-nCoV-RBD induced considerable amounts of protective antibodies against RABV in mice (Fig. 3E). Specifically, the VNAs induced by SRV-nCoV-RBD, reaching a peak with the value of 53.3 IU/mL at 6 weeks after the first immunization, were significantly higher than that of SRV-nCoV-S1 at 6 and 8 weeks.

3.4. Early activation of DCs and B cells in mice post immunization

To verify the cellular immune response induced by the recombinant viruses, mouse lymphocytes from LNs were collected at 3, 6, and 9 days after the first immunization, and the activation of DCs and B cells was analyzed by flow cytometry. The gating strategies for flow cytometry analysis are shown in Supplementary Fig. S1. The results showed that the percentage of $CD11c^{+}$ MHC II^{+} double-positive cells was significantly increased on the 6th and 9th days after immunization with the recombinant viruses compared to the control group (Fig. 4A), and the percentage of $CD11c^{+}$ $CD80^{+}$ double-positive cells was significantly increased on the 6th day after immunization, indicating that the recombinant viruses enhanced the activation of DCs in LNs (Fig. 4B). Compared to the control group, the proportion of $CD19^{+}$ $CD69^{+}$ double-positive cells was significantly increased on the 9th day after immunization with the recombinant viruses, indicating that the recombinant viruses induced the activation of B cells in LNs (Fig. 4C). These data suggested that at the early stage post-immunization, antigens, including inactivated SRV-nCoV-S1 and

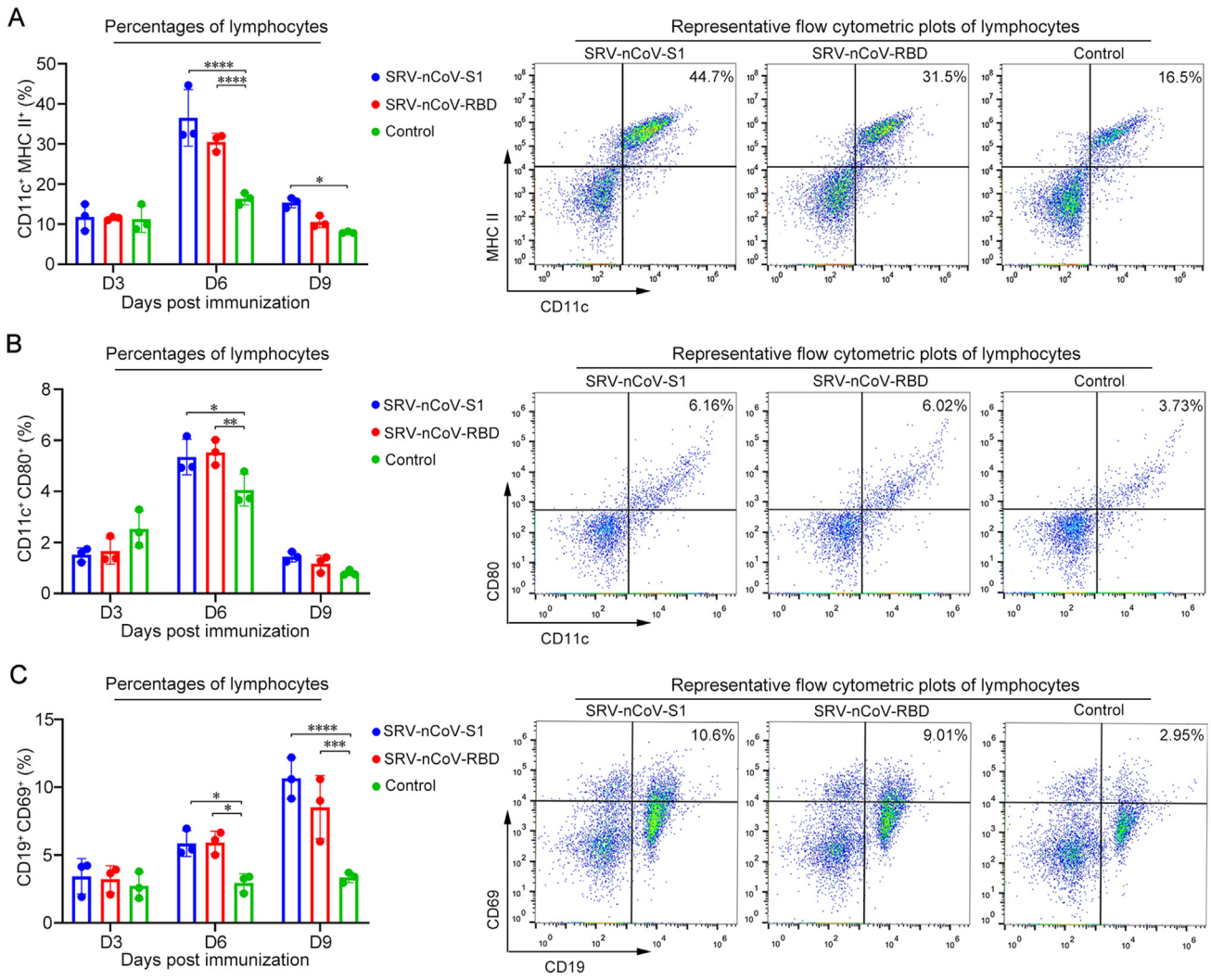

Fig. 4. DC and B-cell activation in mice immunized with recombinant viruses. BALB/c mice were immunized with inactivated recombinant viruses or PBS combined with an adjuvant complex of ISA 201 VG and poly(I:C), respectively. The lymph nodes (LNs) of immunized mice (n = 3/group/day) were collected on days 3, 6 and 9. Single-cell suspensions prepared from LNs were analyzed for the presence of DCs ($CD11c^+$ and $MHC\ II^+$ (**A**) or $CD11c^+$ and $CD80^+$ (**B**) and B cells ($CD19^+$ and $CD69^+$) (**C**). Data are presented as the means ± SD for each group. $^*P < 0.05$; $^{**}P < 0.01$; $^{***}P < 0.001$; $^{****}P < 0.0001$.

SRV-nCoV-RBD, were successfully taken up by DCs in LNs to trigger the activation of DCs followed by the activation of B cells.

3.5. Cytokine secretion upon ex vivo re-stimulation

Cytokines secreted by activated T cells play important roles in regulating the immune response against pathogens (Chabalgoity et al., 2007; Huang et al., 2017). Splenocytes isolated from immunized mice were stimulated with purified SARS-CoV-2 RBD protein and analyzed by ELISpot assay and ELISA to quantify their capacity to produce cytokines. Representative pots of ELISpot assay are shown in Supplementary Fig. S2. The ELISpot results showed that the number of SFCs was significantly increased in the groups immunized with SRV-nCoV-S1 and SRV-nCoV-RBD compared to the control group, indicating that significantly higher levels of IFN-γ (Th1-type cytokine) and IL-4 (Th2-type cytokine) were produced in response to re-stimulation in the vaccinated groups (Fig. 5A). Consistent with the results of the ELISpot assay, the levels of Th1-type (IL-2, TNF-α, and IFN-γ) and Th2-type (IL-4, IL-5, and IL-6) cytokines in the supernatants were significantly higher in the groups vaccinated with SRV-nCoV-S1 and SRV-nCoV-RBD than the control group (Fig. 5B). These data indicated that the inactivated vaccines SRV-nCoV-S1 and SRV-nCoV-RBD promoted the activation of immune cells and subsequently the production of Th1- and Th2-type cytokines *in vivo*.

3.6. T cell memory induced by the recombinant viruses in mice

TCM cells are generated from naive T cells stimulated by antigens as long-term memory T cells that return to LNs to undergo antigen re-stimulation and provide rapid protection. TCM cells are primarily located in the LN, blood, and spleen. To detect the immunological memory induced by the recombinant viruses in mice, splenic lymphocytes isolated from immunized mice one week after the third immunization were stimulated with purified SARS-CoV-2 RBD protein and analyzed by flow cytometry. The results showed that the percentages of $CD62L^+$ $CD44^+$ double-positive cells among $CD4^+$ T cells were significantly increased in the inactivated virus groups compared to the control group (Fig. 6A), and the percentages of $CD62L^+$ $CD44^+$ double-positive cells among $CD8^+$ T cells showed no significant change (Fig. 6B). These results indicated that both inactivated SRV-nCoV-S1 and SRV-nCoV-RBD induced the production of $CD4^+$ TCM cells but not $CD8^+$ TCM cells in mice post immunization.

3.7. Inactivated recombinant SRV-nCoV-RBD induced robust humoral immunity to both SARS-CoV-2 and RABV in cats and dogs

Because the humoral immunity induced by the inactivated vaccine SRV-nCoV-RBD was stronger and lasted longer than the inactivated

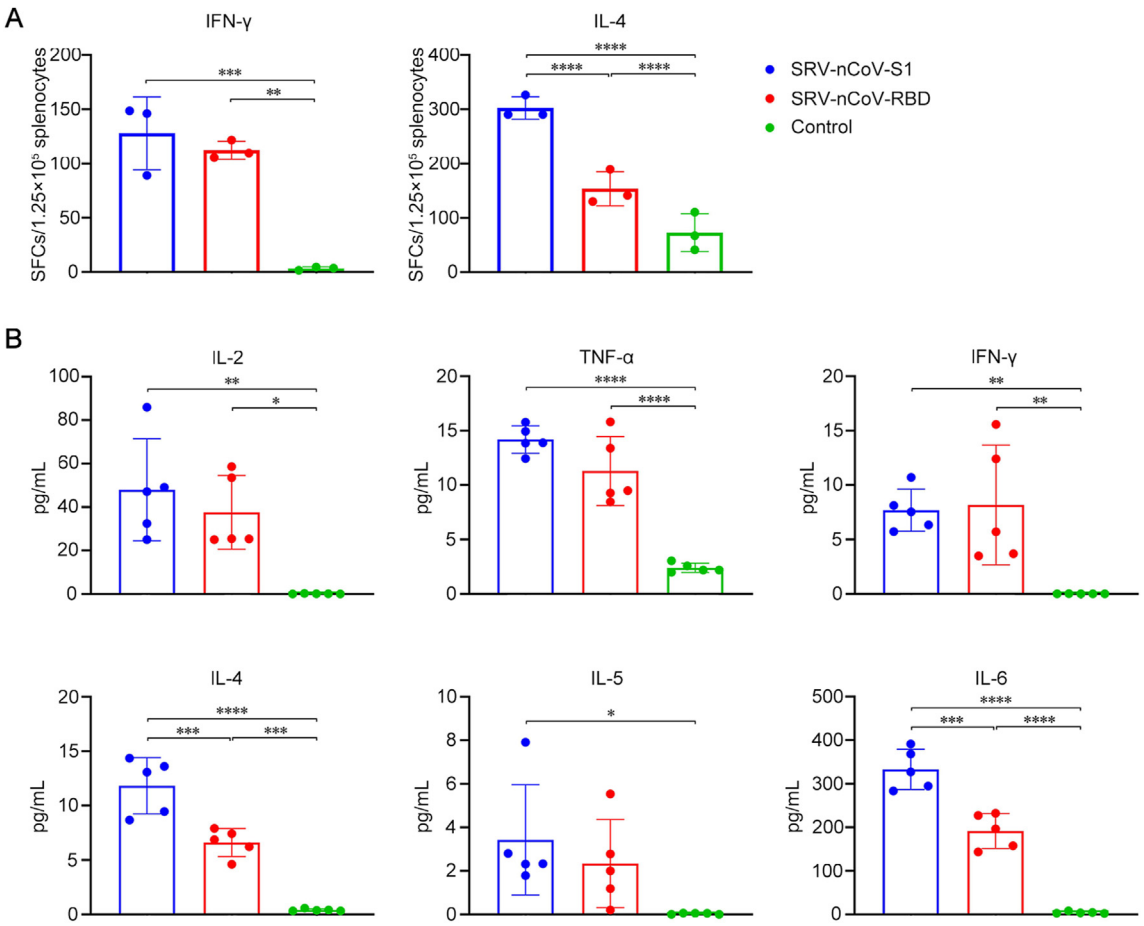

Fig. 5. The cytokine production of activated splenic lymphocytes. On the 35th day post-immunization, splenic lymphocytes from the immunized mice were prepared and stimulated with purified SARS-CoV-2 RBD protein. **A** After *ex vivo* culture for 24 h, the numbers of splenic lymphocytes of immunized mice (n = 3/group) capable of secreting IFN-γ or IL-4 were quantified by an ELISpot assay. **B** After cultured for 72 h, the cytokines in supernatants secreted by splenic lymphocytes of immunized mice (n = 5/group) were measured by MesoScale Discovery (MSD). Data are presented as the means ± SD for each group. $^{*}P < 0.05$; $^{**}P < 0.01$; $^{***}P < 0.001$; $^{****}P < 0.0001$.

SRV-nCoV-S1 in mice (Fig. 3), we chose SRV-nCoV-RBD for further testing of immunogenicity in cats and dogs (Fig. 7). The immunization programs followed the schematic diagram (Fig. 7A and D). No abnormal behavior was observed in cats or dogs immunized with the inactivated SRV-nCoV-RBD during the experiments. IgG antibodies against the SARS-CoV-2 RBD protein were detectable in the sera of the vaccinated group and significantly increased after the booster immunization. The antibodies, with high titers, lasted at least 13 weeks in cats and 11 weeks in dogs after the first immunization (Fig. 7B and E). The titers of VNAs of RABV induced by inactivated SRV-nCoV-RBD were much higher than 0.5 IU/mL and were sustained at a high level for at least 13 weeks in cats and 11 weeks in dogs, indicating that inactivated SRV-nCoV-RBD can robustly induced the production of protective antibodies against RABV in cats and dogs (Fig. 7C and F). These results suggested that the inactivated recombinant SRV-nCoV-RBD induced antibodies against SARS-CoV-2 in cats and dogs and high levels of neutralizing antibodies against RABV.

3.8. Inactivated recombinant virus SRV-nCoV-RBD-induced antibodies exhibit broad cross-neutralizing activity against SARS-CoV-2 variants

To further evaluate the humoral immune responses induced by inactivated recombinant SRV-nCoV-RBD in different animals, we collected sera from mice and cats at six weeks after the first immunization and from dogs at five weeks after the first immunization and tested their neutralization efficiency against different VSV-vectored pseudoviruses of SARS-CoV-2 variants, including Wuhan01, Alpha, Beta, Gamma, Delta, and Omicron (Fig. 8). The neutralizing antibody titer was defined as the highest dilution of sera that completely inhibited virus-caused CPE. The results showed that sera from immunized mice (Fig. 8A) and dogs (Fig. 8C) neutralized Wuhan01, Alpha, Beta, Gamma, and Delta, and to a lesser extent, Omicron. Sera from immunized cats showed neutralization capacity for Wuhan01, Alpha, and Beta, and to a lesser extent, Gamma, Delta, and Omicron (Fig. 8B). These results indicated that the inactivated recombinant SRV-nCoV-RBD could induce the production of neutralizing antibodies in different animals and elicit cross-variant neutralization against most SARS-CoV-2 variants.

4. Discussion

A growing number of studies suggest that SARS-CoV-2 is transmissible between animals and humans, and it poses a certain threat. There is an urgent need to develop inexpensive and efficient animal vaccines to prevent and control COVID-19 in animals to help realize the goal of "One Health". The present study selected RABV as the viral vector to construct a recombinant vector vaccine for COVID-19. The use of RABV as a vaccine vector has many advantages for the construction of recombinant viruses based on its mature reverse genetic system (Schnell et al., 1994; McGettigan et al., 2003), such as a simple genome, permitting the insertion of large fragments of exogenous genes, and lack of integration into the host genome. RABV-vectored vaccines have been developed for a variety of severe diseases and animal diseases (Willet et al., 2015; da Fontoura Budaszewski et al., 2017; Wirblich et al., 2017;

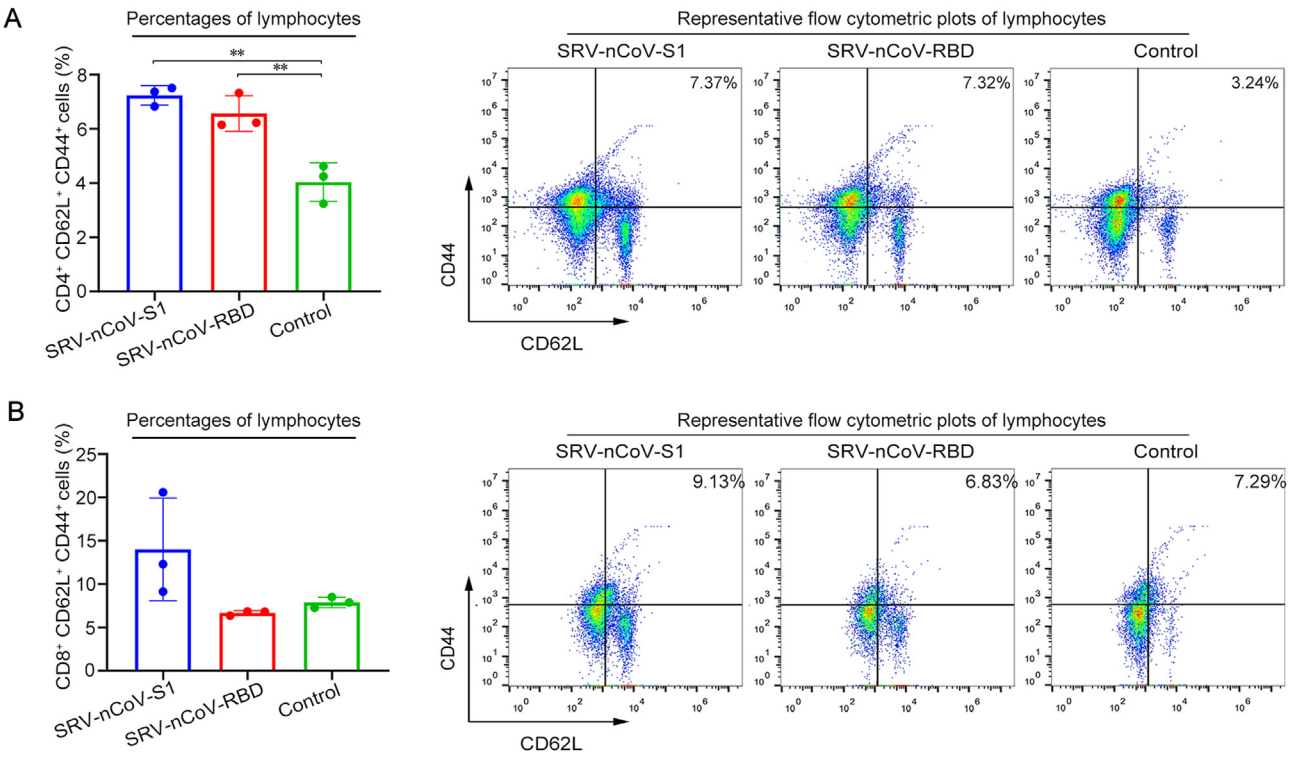

Fig. 6. T cell memory induced by the recombinant viruses in mice. On the 35th day post-immunization, the splenic lymphocytes from the immunized mice (n = 3/group) were prepared and stimulated with purified SARS-CoV-2 RBD protein. After cultured *ex vivo* for 72 h, the percentages of $CD4^+$ TCM cells among $CD4^+$ T cells (**A**) and $CD8^+$ TCM cells among $CD8^+$ T cells (**B**) were assessed by the presence of CD44 and CD62L surface markers. Data are presented as the means ± SD for each group. $^{**}P < 0.01$.

Abreu-Mota et al., 2018; Kurup et al., 2021). The RABV SRV9 strain used in this study was purified from the RABV SAD strain and showed no pathogenicity to a variety of animals (Wang et al., 2015). The recombinant virus constructed based on SRV9 can replicate well in suspended cells to a high titer, which is conducive to mass production and preparation of vaccines in the later stage (Wang et al., 2015). Moreover, the chimeric expression strategy we used here achieved the display of SARS-CoV-2 S1 and RBD proteins on the surface of RABV particles to maintain their conformational structure and enhanced the host immune response when they were used as inactivated vaccines, which avoided the interference of prestored antibodies in animals. Rabies is another important zoonotic disease that endangers animal health, and vaccination remains the only main way to prevent and control rabies. Strengthening animal rabies vaccination, especially vaccination for pet cats and dogs, is an important means to effectively control human rabies (Wallace et al., 2017). The inactivated recombinant SARS-CoV-2 vaccine based on RABV can prevent the spread of the COVID-19 pandemic and effectively control rabies in animals.

The selection of immunogens plays a decisive role in the successful development of vaccines, and ideal immunogens should simultaneously stimulate sustained humoral and cellular immunity (Dai and Gao, 2021). Similar to other coronaviruses, the S protein of SARS-CoV-2 mediates viral entry into cells, and it is widely distributed on the surface of viral particles (Ou et al., 2020). The S protein stimulates high-intensity humoral and cellular immune responses. Further study revealed that the S protein was composed of S1 and S2 proteins. The C-terminal RBD of S1 mediates virus binding to angiotensin-converting enzyme 2 (ACE2), which is the target for neutralizing antibodies (Shi et al., 2020; Wrapp et al., 2020). Therefore, the S1 protein and its RBD are the main immunogen targets for many COVID-19 vaccines (Li et al., 2022). A recent study described the construction of an inactivated vaccine, CORAVAX, that chimerically expressed the S1 protein based on the RABV vector, and this inactivated vaccine induced the production of high levels of neutralizing antibodies against SARS-CoV-2 (Kurup et al., 2020) and prevented disease in a Syrian hamster model (Kurup et al., 2021). The present study constructed two recombinant RABV viruses chimerically expressing S1 and RBD respectively (Figs. 1 and 2), and evaluated their immunogenicity in mice. The results showed that both recombinant viruses induced the production of highly effective SARS-CoV-2 IgG and neutralizing antibodies and RABV-neutralizing antibodies (Fig. 3). Both recombinant viruses induced the activation of DCs and enhanced the uptake and presentation of antigens (Fig. 4), which is an important event in inducing humoral and cellular immunity after vaccination. After the maturation of DCs, Th0 cells can be promote to differentiate into Th1 and Th2 subsets (Vieira et al., 2000), and the secretion of cytokines, including IL-2, TNF-α, IFN-γ, IL-4, IL-5, and IL-6, was significantly increased in the vaccine-immunized groups (Fig. 5), which could provide sufficient protection against SARS-CoV-2 and RABV and in turn affect the differentiation of memory T cells (Chabalgoity et al., 2007). Our results showed that $CD4^+$ TCMs were strongly enriched in the vaccine-immunized groups (Fig. 6), which can provide long-term protection against pathogens and proliferate quickly and secrete cytokines to resist pathogen re-infection (Sahin et al., 2020; Guo et al., 2022). Specifically, inactivated SRV-nCoV-RBD induced the production of antibodies against SARS-CoV-2 and RABV earlier and maintained titers at high levels for a longer time. SRV-nCoV-RBD induced the production of Th1/Th2 balanced antibodies, and SRV-nCoV-S1 induced the production of the Th2-biased antibodies. The Th1 immune response is beneficial for protection against COVID-19 and rabies (Chen et al., 2019; Allegra et al., 2020), and SRV-nCoV-RBD induced the production of higher titers of neutralizing antibodies against SARS-CoV-2 and RABV than SRV-nCoV-S1 (Fig. 3). Therefore, SRV-nCoV-RBD was selected as a vaccine candidate for further immunogenicity testing in cats and dogs. The results showed that this recombinant virus induced the production of neutralizing antibodies against both viruses in cats and dogs (Fig. 7).

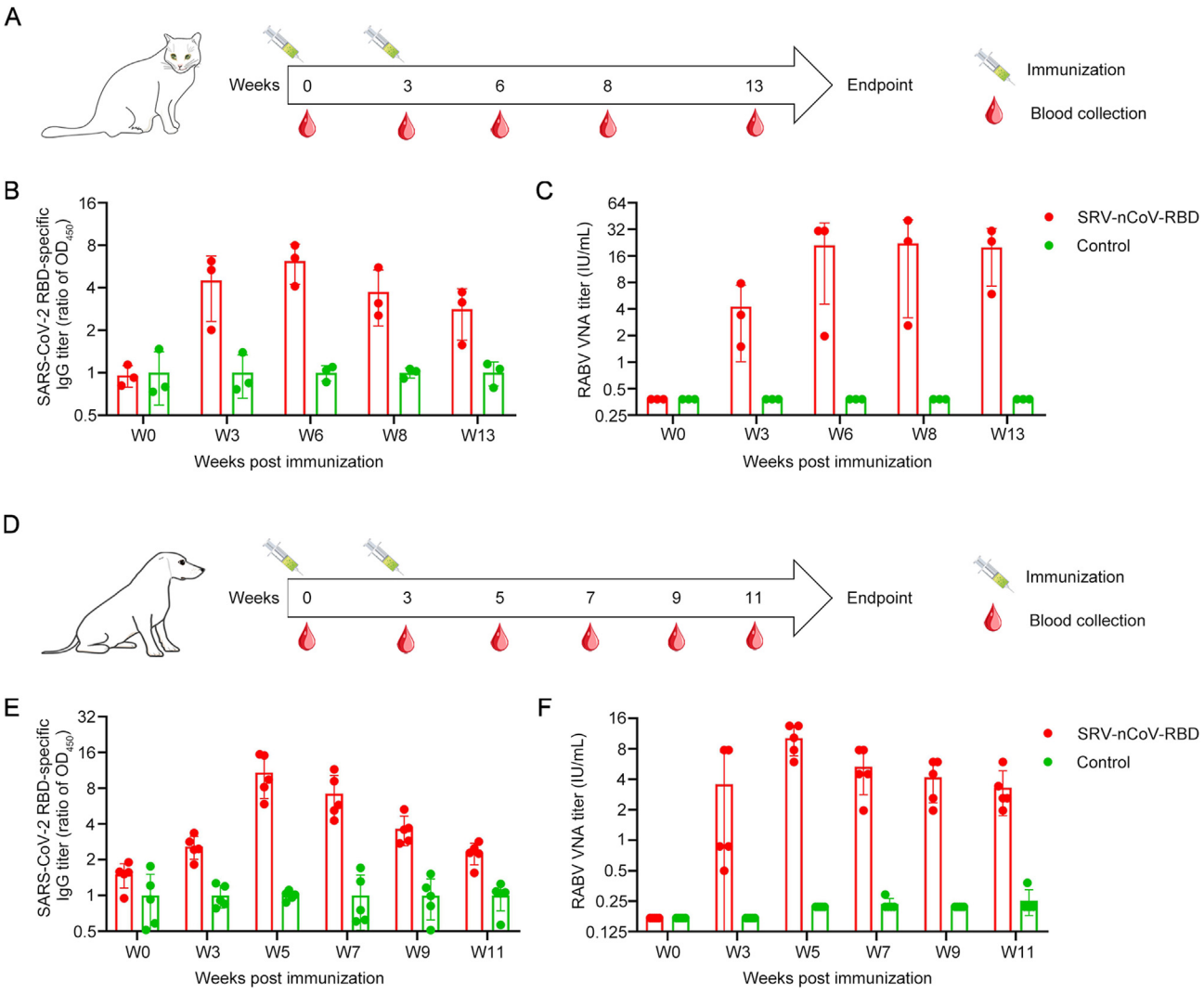

Fig. 7. The inactivated recombinant SRV-nCoV-RBD induced robust humoral immunity to SARS-CoV-2 and RABV in cats and dogs. (**A and D**) Schematic of the immunization strategy in cats (**A**) and dogs (**D**). The cats (n = 3/group) or dogs (n = 5/group) were immunized subcutaneously with two doses of 1 mL of inactivated recombinant viruses or PBS, combined with Gel 02 adjuvant at 3-week intervals. Blood samples were collected at the indicated time points. (**B and E**) SARS-CoV-2 RBD-specific IgG titers of cat sera (**B**) and dog sera (**E**) were detected by indirect ELISA with the purified RBD protein and were displayed as the ratio of sample/control OD_{450}. (**C and F**) RABV-neutralizing antibody titers of cat sera (**C**) and dog sera (**F**) at the indicated time points were determined by the FAVN test. These data are presented as the mean ± SD for each group.

With new VOCs constantly emerging, the accumulation of major antigen site mutations may lead to the immune escape of new mutant strains (Lou et al., 2021; Thomson et al., 2021), which increases the difficulty of pandemic control and brings new challenges to the development of COVID-19 vaccines. A recent study suggested that the sera from individuals naturally infected with the Wuhan01 ancestral strain conferred effective protection against the Wuhan01, Alpha, and Delta, but not the Beta or Omicron strains, showing a relatively broad range of neutralizing activity (Suryawanshi et al., 2022). SRV-nCoV-RBD chimerically expressed RBD of Wuhan01 exhibited varying neutralization titers for VSV-vectored pseudoviruses expressing the intact S protein of SARS-CoV-2 VOCs in this study and showed a wide range of neutralization capabilities (Fig. 8), which is consistent with a previous study (Suryawanshi et al., 2022). Several studies showed that the pseudovirus may be used as an alternative to the authentic viruses for neutralizing antibody detection, and the detection results are highly consistent (Nie et al., 2020; Weisblum et al., 2020; Collier et al., 2021). Although the challenge protection efficiency of this recombinant virus was not measured, we speculated that the recombinant SRV-nCoV-RBD has potential for use as a vaccine candidate against SARS-CoV-2 VOCs and new emerging variants, according to our data. One limitation of the use of this recombinant virus as a vaccine candidate is that the RBD of the ancestral strain, but not the new emerging VOCs, such as Delta or Omicron strains, was chimeric expressed, which may weaken the effectiveness of this vaccine candidate in further application. However, other studies showed that sequential vaccination with heterologous vaccines induced a stronger immune response (Cheng et al., 2022; Lassauniere et al., 2022), and subunit vaccines developed based on the RBD-dimer framework provided broader protection (Xu et al., 2022). Therefore, we will construct more RABV-vectored recombinant viruses to chimerically express the RBD proteins of SARS-CoV-2 VOCs in future work and combine these new recombinant viruses with SRV-nCoV-RBD to develop effective immunization strategies for the control of COVID-19 and rabies in animals.

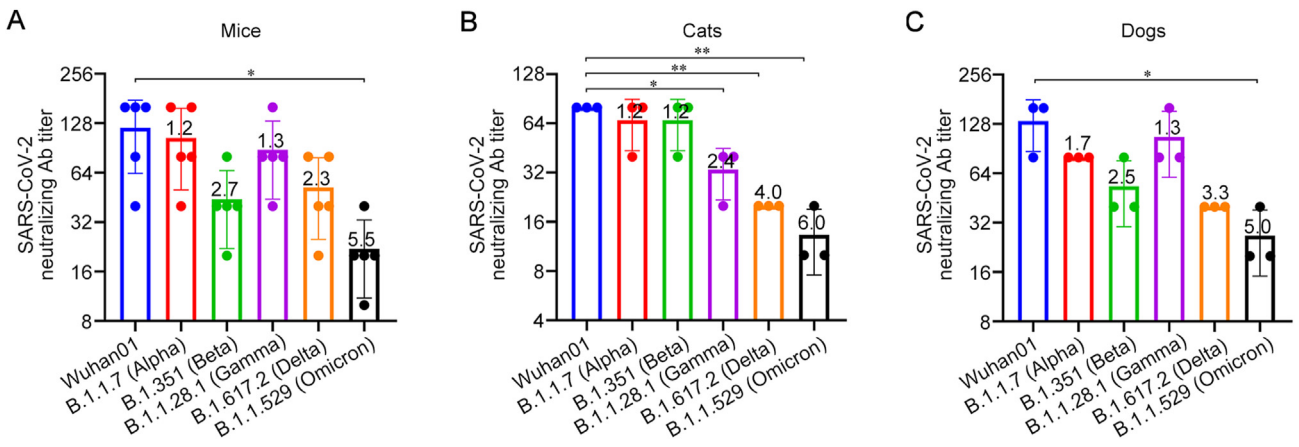

Fig. 8. Inactivated recombinant virus SRV-nCoV-RBD-induced antibodies exhibit broad cross-neutralizing activity against SARS-CoV-2 variants. The sera of mice (n = 5) and cats (n = 3) were collected at six weeks post-immunization and the sera of dogs (n = 3) were collected at five weeks post-immunization. The neutralization titers of mouse sera (**A**), cat sera (**B**), and dog sera (**C**) against different SARS-CoV-2 pseudotyped viruses were determined, including Wuhan01, Alpha, Beta, Gamma, Delta, and Omicron. $^{*}P < 0.05$; $^{**}P < 0.01$. The numbers on the columns represent the fold reduction of neutralizing antibody titer for each variant compared to the Wuhan01 strain.

5. Conclusions

In summary, we constructed an inactivated recombinant virus SRV-nCoV-RBD, based on the RABV vector, which induced humoral and cellular immunity in mice, cats, and dogs with a relatively wide cross-neutralization of variants including Alpha, Beta, Gamma, Delta, and Omicron. This inactivated recombinant virus is a potential bivalent vaccine candidate for the control of COVID-19 and rabies in animals. As the inactivated RABV vaccine has been tested in humans and exhibited high safety, the use of this vaccine candidate in humans cannot be excluded in the future.

Data availability

All of the data generated during the current study are included in the manuscript.

Ethics statement

All of the mice, cats, and dogs, were treated in accordance with the Chinese ethical guidelines for the welfare of laboratory animals (GB 14925-2010). The study was approved by the animal experimental committee of the Laboratory Animal Center, Changchun Veterinary Research Institute (Approval number: IACUC of AMMS-11-2020-020).

Author contributions

Haili Zhang: investigation, formal analysis, data curation, writing-original draft preparation. Hongli Jin: conceptualization, methodology, investigation, formal analysis, data curation, software, writing – review and editing. Feihu Yan: methodology, investigation, formal analysis, data curation. Yumeng Song: methodology, formal analysis, validation. Jiaxin Dai: methodology, formal analysis, validation. Cuicui Jiao: methodology, formal analysis, data curation. Yujie Bai: methodology, formal analysis, data curation. Jingxuan Sun: methodology, formal analysis, data curation. Di Liu: methodology, formal analysis. Shen Wang: methodology. Mengyao Zhang: methodology. Jilong Lu: methodology. Jingbo Huang: methodology. Pei Huang: methodology. Yuanyuan Li: funding acquisition, resources. Xianzhu Xia: resources. Hualei Wang: conceptualization, data curation, formal analysis, funding acquisition, investigation, project administration, resources, software, supervision, writing – review and editing.

Conflict of interest

The authors declare no conflicts of interest, financial or otherwise.

Acknowledgements

This research was funded by the National Key Research and Development Program of China (grant No. 2021YFC2600202) and the National Natural Science Foundation of China (grant numbers 31872487).

Appendix A. Supplementary data

Supplementary data to this article can be found online at https://doi.org/10.1016/j.virs.2022.12.006.

References

Abreu-Mota, T., Hagen, K.R., Cooper, K., Jahrling, P.B., Tan, G., Wirblich, C., Johnson, R.F., Schnell, M.J., 2018. Non-neutralizing antibodies elicited by recombinant lassa-rabies vaccine are critical for protection against lassa fever. Nat. Commun. 9, 4223.

Ahmad, W., Li, Y., Guo, Y., Wang, X., Duan, M., Guan, Z., Liu, Z., Zhang, M., 2017. Rabies virus co-localizes with early (Rab5) and late (Rab7) endosomal proteins in neuronal and SH-SY5Y cells. Virol. Sin. 32, 207–215.

Allegra, A., Di Gioacchino, M., Tonacci, A., Musolino, C., Gangemi, S., 2020. Immunopathology of SARS-CoV-2 infection: immune cells and mediators, prognostic factors, and immune-therapeutic implications. Int. J. Mol. Sci. 21, 4782.

Andrianaivoarimanana, V., Telfer, S., Rajerison, M., Ranjalahy, M.A., Andriamiarimanana, F., Rahaingosoamamitiana, C., Rahalison, L., Jambou, R., 2012. Immune responses to plague infection in wild rattus rattus, in Madagascar: a role in foci persistence? PLoS One 7, e38630.

Chabalgoity, J.A., Baz, A., Rial, A., Grille, S., 2007. The relevance of cytokines for development of protective immunity and rational design of vaccines. Cytokine Growth Factor Rev. 18, 195–207.

Chan, J.F., Siu, G.K., Yuan, S., Ip, J.D., Cai, J.P., Chu, A.W., Chan, W.M., Abdullah, S.M.U., Luo, C., Chan, B.P., Yuen, T.T., Chen, L.L., Chik, K.K., Liang, R., Cao, H., Man Poon, V.K., Chan, C.C., Leung, K.H., Tam, A.R., Tsang, O.T., Chan, J.M., To, W.K., Lam, B.H., Lee, L.K., Lo, H.W., Wong, I.T., Leung, J.S., Wong, E.Y., Chu, H., Yip, C.C., Cheng, V.C., Chan, K.H., Tse, H., Lung, D.C., Ng, K.H., Au, A.K., Hung, I.F., Yuen, K.Y., To, K.K., 2022. Probable animal-to-human transmission of SARS-CoV-2 delta variant AY.127 causing a pet shop-related COVID-19 outbreak in Hong Kong. Clin. Infect. Dis. 75, e76–e81.

Chen, C., Zhang, C.G., Li, R.M., Wang, Z.M., Yuan, Y.M., Li, H.Q., Fu, Z.F., Zhou, M., Zhao, L., 2019. In: Monophosphoryl-lipid a (mpla) Is an Efficacious Adjuvant for Inactivated Rabies Vaccines. Viruses 11, 1118.

Cheng, S.M.S., Mok, C.K.P., Leung, Y.W.Y., Ng, S.S., Chan, K.C.K., Ko, F.W., Chen, C., Yiu, K., Lam, B.H.S., Lau, E.H.Y., Chan, K.K.P., Luk, L.L.H., Li, J.K.C., Tsang, L.C.H., Poon, L.L.M., Hui, D.S.C., Peiris, M., 2022. Neutralizing antibodies against the SARS-CoV-2 Omicron variant BA.1 following homologous and heterologous coronavac or BNT162b2 vaccination. Nat. Med. 28, 486–489.

Chi, H., Wang, Y., Li, E., Wang, X., Wang, H., Jin, H., Han, Q., Wang, Z., Wang, X., Zhu, A., Sun, J., Zhuang, Z., Zhang, L., Ye, J., Wang, H., Feng, N., Hu, M., Gao, Y., Zhao, J., Zhao, Y., Yang, S., Xia, X., 2022. Inactivated rabies virus vectored MERS-coronavirus vaccine induces protective immunity in mice, camels, and alpacas. Front. Immunol. 13, 823949.

Cliquet, F., Aubert, M., Sagne, L., 1998. Development of a fluorescent antibody virus neutralisation test (FAVN test) for the quantitation of rabies-neutralising antibody. J. Immunol. Methods 212, 79–87.

Collier, D.A., Ferreira, I., Kotagiri, P., Datir, R.P., Lim, E.Y., Touizer, E., Meng, B., Abdullahi, A., Collaboration, C.-N.B.C.-, Elmer, A., Kingston, N., Graves, B., Le Gresley, E., Caputo, D., Bergamaschi, L., Smith, K.G.C., Bradley, J.R., Ceron-Gutierrez, L., Cortes-Acevedo, P., Barcenas-Morales, G., Linterman, M.A., McCoy, L.E., Davis, C., Thomson, E., Lyons, P.A., McKinney, E., Doffinger, R., Wills, M., Gupta, R.K., 2021. Age-related immune response heterogeneity to SARS-CoV-2 vaccine BNT162b2. Nature 596, 417–422.

da Fontoura Budaszewski, R., Hudacek, A., Sawatsky, B., Kramer, B., Yin, X., Schnell, M.J., von Messling, V., 2017. Inactivated recombinant rabies viruses displaying canine distemper virus glycoproteins induce protective immunity against both pathogens. J. Virol. 91, e02077–16.

Dai, L., Gao, G.F., 2021. Viral targets for vaccines against COVID-19. Nat. Rev. Immunol. 21, 73–82.

Gao, Q., Bao, L., Mao, H., Wang, L., Xu, K., Yang, M., Li, Y., Zhu, L., Wang, N., Lv, Z., Gao, H., Ge, X., Kan, B., Hu, Y., Liu, J., Cai, F., Jiang, D., Yin, Y., Qin, C., Li, J., Gong, X., Lou, X., Shi, W., Wu, D., Zhang, H., Zhu, L., Deng, W., Li, Y., Lu, J., Li, C., Wang, X., Yin, W., Zhang, Y., Qin, C., 2020. Development of an inactivated vaccine candidate for SARS-CoV-2. Science 369, 77–81.

Guo, L., Wang, G., Wang, Y., Zhang, Q., Ren, L., Gu, X., Huang, T., Zhong, J., Wang, Y., Wang, X., Huang, L., Xu, L., Wang, C., Chen, L., Xiao, X., Peng, Y., Knight, J.C., Dong, T., Cao, B., Wang, J., 2022. SARS-CoV-2-specific antibody and T-cell responses 1 year after infection in people recovered from COVID-19: a longitudinal cohort study. Lancet Microb. 3, e348–e356.

Hoffmann, M., Zhang, L., Krüger, N., Graichen, L., Kleine-Weber, H., Hofmann-Winkler, H., Kempf, A., Nessler, S., Riggert, J., Winkler, M.S., Schulz, S., Jäck, H.M., Pöhlmann, S., 2021. SARS-CoV-2 mutations acquired in mink reduce antibody-mediated neutralization. Cell Rep. 35, 109017.

Huang, Y., Pantaleo, G., Tapia, G., Sanchez, B., Zhang, L., Trondsen, M., Hovden, A.O., Pollard, R., Rockstroh, J., Okvist, M., Sommerfelt, M.A., 2017. Cell-mediated immune predictors of vaccine effect on viral load and CD4 count in a phase 2 therapeutic HIV-1 vaccine clinical trial. EBioMedicine 24, 195–204.

Jin, H., Jiao, C., Cao, Z., Huang, P., Chi, H., Bai, Y., Liu, D., Wang, J., Feng, N., Li, N., Zhao, Y., Wang, T., Gao, Y., Yang, S., Xia, X., Wang, H., 2021. An inactivated recombinant rabies virus displaying the Zika virus prM-E induces protective immunity against both pathogens. PLoS Neglected Trop. Dis. 15, e0009484.

Jin, H., Bai, Y., Wang, J., Jiao, C., Liu, D., Zhang, M., Li, E., Huang, P., Gong, Z., Song, Y., Xu, S., Feng, N., Zhao, Y., Wang, T., Li, N., Gao, Y., Yang, S., Zhang, H., Li, Y., Xia, X., Wang, H., 2022. A bacterium-like particle vaccine displaying Zika virus prM-E induces systemic immune responses in mice. Transbound. Emer. Dis. 69, e2516–e2529.

Kim, Y.I., Kim, S.G., Kim, S.M., Kim, E.H., Park, S.J., Yu, K.M., Chang, J.H., Kim, E.J., Lee, S., Casel, M.A.B., Um, J., Song, M.S., Jeong, H.W., Lai, V.D., Kim, Y., Chin, B.S., Park, J.S., Chung, K.H., Foo, S.S., Poo, H., Mo, I.P., Lee, O.J., Webby, R.J., Jung, J.U., Choi, Y.K., 2020. Infection and rapid transmission of SARS-CoV-2 in ferrets. Cell Host Microbe 27, 704–709.e702.

Kurup, D., Wirblich, C., Ramage, H., Schnell, M.J., 2020. Rabies virus-based COVID-19 vaccine coravaxTM induces high levels of neutralizing antibodies against SARS-CoV-2. NPJ Vacc. 5, 98.

Kurup, D., Malherbe, D.C., Wirblich, C., Lambert, R., Ronk, A.J., Zabihi Diba, L., Bukreyev, A., Schnell, M.J., 2021. Inactivated rabies virus vectored SARS-CoV-2 vaccine prevents disease in a syrian hamster model. PLoS Pathog. 17, e1009383.

Lassauniere, R., Polacek, C., Frische, A., Boding, L., Saekmose, S.G., Rasmussen, M., Fomsgaard, A., 2022. Neutralizing antibodies against the SARS-CoV-2 Omicron variant (BA.1) 1 to 18 weeks after the second and third doses of the BNT162b2 mrna vaccine. JAMA Netw. Open 5, e2212073.

Li, E., Yan, F., Huang, P., Chi, H., Xu, S., Li, G., Liu, C., Feng, N., Wang, H., Zhao, Y., Yang, S., Xia, X., 2020. Characterization of the immune response of MERS-CoV vaccine candidates derived from two different vectors in mice. Viruses 12, 125.

Li, M., Wang, H., Tian, L., Pang, Z., Yang, Q., Huang, T., Fan, J., Song, L., Tong, Y., Fan, H., 2022. COVID-19 vaccine development: milestones, lessons and prospects. Signal Transduct. Targeted Ther. 7, 146.

Liu, J., Liao, M., Yan, Y., Yang, H., Wang, H., Zhou, J., 2020. Rabies virus phosphoprotein P5 binding to BECN1 regulates self-replication by BECN1-mediated autophagy signaling pathway. Cell Commun. Signal. 18, 153.

Lou, F., Li, M., Pang, Z., Jiang, L., Guan, L., Tian, L., Hu, J., Fan, J., Fan, H., 2021. Understanding the secret of SARS-CoV-2 variants of concern/interest and immune escape. Front. Immunol. 12, 744242.

Lourenc Correia Moreira, B., Aparecida Pereira, L., Lappas Gimenez, A.P., Minor Fernandes Inagaki, J., Raboni, S.M., 2019. Development and validation of a real-time RT-PCR assay for the quantification of rabies virus as quality control of inactivated rabies vaccines. J. Virol Methods 270, 46–51.

Lundstrom, K., 2020. Application of viral vectors for vaccine development with a special emphasis on COVID-19. Viruses 12, 1324.

Maruggi, G., Zhang, C., Li, J., Ulmer, J.B., Yu, D., 2019. mRNA as a transformative technology for vaccine development to control infectious diseases. Mol. Ther. 27, 757–772.

McAloose, D., Laverack, M., Wang, L., Killian, M.L., Caserta, L.C., Yuan, F., Mitchell, P.K., Queen, K., Mauldin, M.R., Cronk, B.D., Bartlett, S.L., Sykes, J.M., Zec, S., Stokol, T., Ingerman, K., Delaney, M.A., Fredrickson, R., Ivančić, M., Jenkins-Moore, M., Mozingo, K., Franzen, K., Bergeson, N.H., Goodman, L., Wang, H., Fang, Y., Olmstead, C., McCann, C., Thomas, P., Goodrich, E., Elvinger, F., Smith, D.C., Tong, S., Slavinski, S., Calle, P.P., Terio, K., Torchetti, M.K., Diel, D.G., 2020. From people to panthera: Natural SARS-CoV-2 infection in tigers and lions at the Bronx zoo. mBio 11, e02220–20.

McGettigan, J.P., Naper, K., Orenstein, J., Koser, M., McKenna, P.M., Schnell, M.J., 2003. Functional human immunodeficiency virus type 1 (HIV-1) gag-pol or HIV-1 gag-pol and env expressed from a single rhabdovirus-based vaccine vector genome. J. Virol. 77, 10889–10899.

Muench, H., Reed, L., 1938. A Simple Method of Estimating Fifty Percent Endpoints. Am. J. Epidemiol. 27, 493–497.

Mulligan, M.J., Lyke, K.E., Kitchin, N., Absalon, J., Gurtman, A., Lockhart, S., Neuzil, K., Raabe, V., Bailey, R., Swanson, K.A., Li, P., Koury, K., Kalina, W., Cooper, D., Fontes-Garfias, C., Shi, P.Y., Türeci, Ö., Tompkins, K.R., Walsh, E.E., Frenck, R., Falsey, A.R., Dormitzer, P.R., Gruber, W.C., Şahin, U., Jansen, K.U., 2020. Phase I/II study of COVID-19 RNA vaccine BNT162b1 in adults. Nature 586, 589–593.

Munnink, B.B.O., Sikkema, R.S., Nieuwenhuijse, D.F., Molenaar, R.J., Munger, E., Molenkamp, R., van der Spek, A., Tolsma, P., Rietveld, A., Brouwer, M., Bouwmeester-Vincken, N., Harders, F., Hakze-van der Honing, R., Wegdam-Blans, M.C.A., Bouwstra, R.J., GeurtsvanKessel, C., van der Eijk, A.A., Velkers, F.C., Smit, L.A.M., Stegeman, A., van der Poel, W.H.M., Koopmans, M.P.G., 2021. Transmission of SARS-CoV-2 on mink farms between humans and mink and back to humans. Science 371, 172–177.

Nie, J., Li, Q., Wu, J., Zhao, C., Hao, H., Liu, H., Zhang, L., Nie, L., Qin, H., Wang, M., Lu, Q., Li, X., Sun, Q., Liu, J., Fan, C., Huang, W., Xu, M., Wang, Y., 2020. Establishment and validation of a pseudovirus neutralization assay for SARS-CoV-2. Emerg. Microb. Infect. 9, 680–686.

Ou, X., Liu, Y., Lei, X., Li, P., Mi, D., Ren, L., Guo, L., Guo, R., Chen, T., Hu, J., Xiang, Z., Mu, Z., Chen, X., Chen, J., Hu, K., Jin, Q., Wang, J., Qian, Z., 2020. Characterization of spike glycoprotein of SARS-CoV-2 on virus entry and its immune cross-reactivity with SARS-CoV. Nat. Commun. 11, 1620.

Phillips, P.L., Reyes, L., Sampson, E.M., Murrell, E.A., Whitlock, J.A., Progulske-Fox, A., 2018. Deletion of a conserved transcript PG_RS02100 expressed during logarithmic growth in Porphyromonas gingivalis results in hyperpigmentation and increased tolerance to oxidative stress. PLoS One 13, e0207295.

Sahin, U., Muik, A., Derhovanessian, E., Vogler, I., Kranz, L.M., Vormehr, M., Baum, A., Pascal, K., Quandt, J., Maurus, D., Brachtendorf, S., Lorks, V., Sikorski, J., Hilker, R., Becker, D., Eller, A.K., Grutzner, J., Boesler, C., Rosenbaum, C., Kuhnle, M.C., Luxemburger, U., Kemmer-Bruck, A., Langer, D., Bexon, M., Bolte, S., Kariko, K., Palanche, T., Fischer, B., Schultz, A., Shi, P.Y., Fontes-Garfias, C., Perez, J.L., Swanson, K.A., Loschko, J., Scully, I.L., Cutler, M., Kalina, W., Kyratsous, C.A., Cooper, D., Dormitzer, P.R., Jansen, K.U., Tureci, O., 2020. COVID-19 vaccine BNT162b1 elicits human antibody and Th1 T cell responses. Nature 586, 594–599.

Schnell, M.J., Mebatsion, T., Conzelmann, K.K., 1994. Infectious rabies viruses from cloned cDNA. EMBO J. 13, 4195–4203.

Shi, J., Wen, Z., Zhong, G., Yang, H., Wang, C., Huang, B., Liu, R., He, X., Shuai, L., Sun, Z., Zhao, Y., Liu, P., Liang, L., Cui, P., Wang, J., Zhang, X., Guan, Y., Tan, W., Wu, G., Chen, H., Bu, Z., 2020. Susceptibility of ferrets, cats, dogs, and other domesticated animals to SARS-coronavirus 2. Science 368, 1016–1020.

Shi, R., Shan, C., Duan, X., Chen, Z., Liu, P., Song, J., Song, T., Bi, X., Han, C., Wu, L., Gao, G., Hu, X., Zhang, Y., Tong, Z., Huang, W., Liu, W.J., Wu, G., Zhang, B., Wang, L., Qi, J., Feng, H., Wang, F.S., Wang, Q., Gao, G.F., Yuan, Z., Yan, J., 2020. A human neutralizing antibody targets the receptor-binding site of SARS-CoV-2. Nature 584, 120–124.

Shiota, S., Mannen, K., Matsumoto, T., Yamada, K., Yasui, T., Takayama, K., Kobayashi, Y., Khawplod, P., Gotoh, K., Ahmed, K., Iha, H., Nishizono, A., 2009. Development and evaluation of a rapid neutralizing antibody test for rabies. J. Virol Methods 161, 58–62.

Sila, T., Sunghan, J., Laochareonsuk, W., Surasombatpattana, S., Kongkamol, C., Ingviya, T., Siripaitoon, P., Kositpantawong, N., Kanchanasuwan, S., Hortiwakul, T., Charernmak, B., Nwabor, O.F., Silpapojakul, K., Chusri, S., 2022. Suspected cat-to-human transmission of SARS-CoV-2, Thailand, July-September 2021. Emerg. Infect. Dis. 28, 1485–1488.

Suryawanshi, R.K., Chen, I.P., Ma, T., Syed, A.M., Brazer, N., Saldhi, P., Simoneau, C.R., Ciling, A., Khalid, M.M., Sreekumar, B., Chen, P.Y., Kumar, G.R., Montano, M., Gascon, R., Tsou, C.L., Garcia-Knight, M.A., Sotomayor-Gonzalez, A., Servellita, V., Gliwa, A., Nguyen, J., Silva, I., Milbes, B., Kojima, N., Hess, V., Shacreaw, M., Lopez, L., Brobeck, M., Turner, F., Soveg, F.W., George, A.F., Fang, X., Maishan, M., Matthay, M., Morris, M.K., Wadford, D., Hanson, C., Greene, W.C., Andino, R., Spraggon, L., Roan, N.R., Chiu, C.Y., Doudna, J.A., Ott, M., 2022. Limited cross-variant immunity from SARS-CoV-2 Omicron without vaccination. Nature 607, 351–355.

Thomson, E.C., Rosen, L.E., Shepherd, J.G., Spreafico, R., Filipe, A.D., Wojcechowskyj, J.A., Davis, C., Piccoli, L., Pascall, D.J., Dillen, J., Lytras, S., Czudnochowski, N., Shah, R., Meury, M., Jesudason, N., De Marco, A., Li, K., Bassi, J., O'Toole, A., Pinto, D., Colquhoun, R.M., Culap, K., Jackson, B., Zatta, F., Rambaut, A., Jaconi, S., Sreenu, V.B., Nix, J., Zhang, I., Jarrett, R.F., Glass, W.G., Beltramello, M., Nomikou, K., Pizzuto, M., Tong, L., Cameroni, E., Croll, T.I., Johnson, N., Di Iulio, J., Wickenhagen, A., Ceschi, A., Harbison, A.M., Mair, D., Ferrari, P., Smollett, K., Sallusto, F., Carmichael, S., Garzoni, C., Nichols, J., Galli, M., Hughes, J., Riva, A., Ho, A., Schiuma, M., Semple, M.G., Openshaw, P.J.M., Fadda, E., Baillie, J.K., Chodera, J.D., Rihn, S.J., Lycett, S.J., Virgin, H.W., Telenti, A., Corti, D., Robertson, D.L., Snell, G., Investigators IC, Consor C-GUC-U, 2021. Circulating SARS-CoV-2 spike N439K variants maintain fitness while evading antibody-mediated immunity. Cell 184, 1171–1187.e20.

van Doremalen, N., Lambe, T., Spencer, A., Belij-Rammerstorfer, S., Purushotham, J.N., Port, J.R., Avanzato, V.A., Bushmaker, T., Flaxman, A., Ulaszewska, M., Feldmann, F., Allen, E.R., Sharpe, H., Schulz, J., Holbrook, M., Okumura, A., Meade-White, K., Pérez-Pérez, L., Edwards, N.J., Wright, D., Bissett, C., Gilbride, C., Williamson, B.N., Rosenke, R., Long, D., Ishwarbhai, A., Kailath, R., Rose, L., Morris, S., Powers, C., Lovaglio, J., Hanley, P.W., Scott, D., Saturday, G., de Wit, E., Gilbert, S.C., Munster, V.J., 2020. Chadox1 nCoV-19 vaccine prevents SARS-CoV-2 pneumonia in rhesus macaques. Nature 586, 578–582.

Vieira, P.L., de Jong, E.C., Wierenga, E.A., Kapsenberg, M.L., Kalinski, P., 2000. Development of Th1-inducing capacity in myeloid dendritic cells requires environmental instruction. J. Immunol. 164, 4507–4512.

Wallace, R.M., Undurraga, E.A., Blanton, J.D., Cleaton, J., Franka, R., 2017. Elimination of dog-mediated human rabies deaths by 2030: needs assessment and alternatives for progress based on dog vaccination. Front. Vet. Sci. 4, 9.

Wang, H., Jin, H., Feng, N., Zheng, X., Li, L., Qi, Y., Liang, M., Zhao, Y., Wang, T., Gao, Y., Tu, C., Jin, N., Yang, S., Xia, X., 2015. Using rabies virus vaccine strain SRV9 as viral vector to express exogenous gene. Virus Gene. 50, 299–302.

Wang, N., Shang, J., Jiang, S., Du, L., 2020. Subunit vaccines against emerging pathogenic human coronaviruses. Front. Microbiol. 11, 298.

Wang, S., Zhang, C., Liang, B., Wang, W., Feng, N., Zhao, Y., Wang, T., Guo, Z., Yan, F., Yang, S., Xia, X., 2022. Characterization of immune response diversity in rodents vaccinated with a vesicular stomatitis virus vectored COVID-19 vaccine. Viruses 14, 1127.

Weisblum, Y., Schmidt, F., Zhang, F., DaSilva, J., Poston, D., Lorenzi, J.C., Muecksch, F., Rutkowska, M., Hoffmann, H.H., Michailidis, E., Gaebler, C., Agudelo, M., Cho, A., Wang, Z., Gazumyan, A., Cipolla, M., Luchsinger, L., Hillyer, C.D., Caskey, M., Robbiani, D.F., Rice, C.M., Nussenzweig, M.C., Hatziioannou, T., Bieniasz, P.D., 2020. Escape from neutralizing antibodies by SARS-CoV-2 spike protein variants. Elife 9, e61312.

Willet, M., Kurup, D., Papaneri, A., Wirblich, C., Hooper, J.W., Kwilas, S.A., Keshwara, R., Hudacek, A., Beilfuss, S., Rudolph, G., Pommerening, E., Vos, A., Neubert, A., Jahrling, P., Blaney, J.E., Johnson, R.F., Schnell, M.J., 2015. Preclinical development of inactivated rabies virus-based polyvalent vaccine against rabies and filoviruses. J. Infect. Dis. 212 (Suppl. 2), S414–S424.

Wirblich, C., Coleman, C.M., Kurup, D., Abraham, T.S., Bernbaum, J.G., Jahrling, P.B., Hensley, L.E., Johnson, R.F., Frieman, M.B., Schnell, M.J., 2017. One-health: a safe, efficient, dual-use vaccine for humans and animals against middle east respiratory syndrome coronavirus and rabies virus. J. Virol. 91, e02040–16.

Wrapp, D., Wang, N., Corbett, K.S., Goldsmith, J.A., Hsieh, C.L., Abiona, O., Graham, B.S., McLellan, J.S., 2020. Cryo-EM structure of the 2019-nCoV spike in the prefusion conformation. Science 367, 1260–1263.

Xia, S., Zhang, Y., Wang, Y., Wang, H., Yang, Y., Gao, G.F., Tan, W., Wu, G., Xu, M., Lou, Z., Huang, W., Xu, W., Huang, B., Wang, H., Wang, W., Zhang, W., Li, N., Xie, Z., Ding, L., You, W., Zhao, Y., Yang, X., Liu, Y., Wang, Q., Huang, L., Yang, Y., Xu, G., Luo, B., Wang, W., Liu, P., Guo, W., Yang, X., 2021. Safety and immunogenicity of an inactivated SARS-CoV-2 vaccine, BBIBP-CorV: a randomised, double-blind, placebo-controlled, phase 1/2 trial. Lancet Infect. Dis. 21, 39–51.

Xu, K., Gao, P., Liu, S., Lu, S., Lei, W., Zheng, T., Liu, X., Xie, Y., Zhao, Z., Guo, S., Tang, C., Yang, Y., Yu, W., Wang, J., Zhou, Y., Huang, Q., Liu, C., An, Y., Zhang, R., Han, Y., Duan, M., Wang, S., Yang, C., Wu, C., Liu, X., She, G., Liu, Y., Zhao, X., Xu, K., Qi, J., Wu, G., Peng, X., Dai, L., Wang, P., Gao, G.F., 2022. Protective Prototype-Beta and Delta-Omicron Chimeric RBD-Dimer Vaccines against SARS-CoV-2. Cell 185, 2265–2278.e14.

Yan, F., Li, E., Wang, T., Li, Y., Liu, J., Wang, W., Qin, T., Su, R., Pei, H., Wang, S., Feng, N., Zhao, Y., Yang, S., Xia, X., Gao, Y., 2022. Characterization of two heterogeneous lethal mouse-adapted SARS-CoV-2 variants recapitulating representative aspects of human COVID-19. Front. Immunol. 13, 821664.

Yang, J., Wang, W., Chen, Z., Lu, S., Yang, F., Bi, Z., Bao, L., Mo, F., Li, X., Huang, Y., Hong, W., Yang, Y., Zhao, Y., Ye, F., Lin, S., Deng, W., Chen, H., Lei, H., Zhang, Z., Luo, M., Gao, H., Zheng, Y., Gong, Y., Jiang, X., Xu, Y., Lv, Q., Li, D., Wang, M., Li, F., Wang, S., Wang, G., Yu, P., Qu, Y., Yang, L., Deng, H., Tong, A., Li, J., Wang, Z., Yang, J., Shen, G., Zhao, Z., Li, Y., Luo, J., Liu, H., Yu, W., Yang, M., Xu, J., Wang, J., Li, H., Wang, H., Kuang, D., Lin, P., Hu, Z., Guo, W., Cheng, W., He, Y., Song, X., Chen, C., Xue, Z., Yao, S., Chen, L., Ma, X., Chen, S., Gou, M., Huang, W., Wang, Y., Fan, C., Tian, Z., Shi, M., Wang, F.S., Dai, L., Wu, M., Li, G., Wang, G., Peng, Y., Qian, Z., Huang, C., Lau, J.Y., Yang, Z., Wei, Y., Cen, X., Peng, X., Qin, C., Zhang, K., Lu, G., Wei, X., 2020. A vaccine targeting the RBD of the S protein of SARS-CoV-2 induces protective immunity. Nature 586, 572–577.

Yen, H.L., Sit, T.H.C., Brackman, C.J., Chuk, S.S.Y., Gu, H., Tam, K.W.S., Law, P.Y.T., Leung, G.M., Peiris, M., Poon, L.L.M., team, H-Ss, 2022. Transmission of SARS-CoV-2 Delta variant (AY.127) from pet hamsters to humans, leading to onward human-to-human transmission: a case study. Lancet 399, 1070–1078.

Zhang, S., Hao, M., Feng, N., Jin, H., Yan, F., Chi, H., Wang, H., Han, Q., Wang, J., Wong, G., Liu, B., Wu, J., Bi, Y., Wang, T., Sun, W., Gao, Y., Yang, S., Zhao, Y., Xia, X., 2019. Genetically modified rabies virus vector-based rift valley fever virus vaccine is safe and induces efficacious immune responses in mice. Viruses 11, 919.

Zhu, F.C., Guan, X.H., Li, Y.H., Huang, J.Y., Jiang, T., Hou, L.H., Li, J.X., Yang, B.F., Wang, L., Wang, W.J., Wu, S.P., Wang, Z., Wu, X.H., Xu, J.J., Zhang, Z., Jia, S.Y., Wang, B.S., Hu, Y., Liu, J.J., Zhang, J., Qian, X.A., Li, Q., Pan, H.X., Jiang, H.D., Deng, P., Gou, J.B., Wang, X.W., Wang, X.H., Chen, W., 2020. Immunogenicity and safety of a recombinant adenovirus type-5-vectored COVID-19 vaccine in healthy adults aged 18 years or older: a randomised, double-blind, placebo-controlled, phase 2 trial. Lancet 396, 479–488.